ELSEVIER

Journal of Marine Systems 35 (2002) 79–97

JOURNAL OF MARINE SYSTEMS

www.elsevier.com/locate/jmarsys

# Spatial variability of chlorophyll-*a* in the Marginal Ice Zone of the Barents Sea, with relations to sea ice and oceanographic conditions

Ola Engelsen [a,*], Else Nøst Hegseth [b], Haakon Hop [a], Edmond Hansen [a], Stig Falk-Petersen [a]

[a] *Norwegian Polar Institute, N-9296 Tromsø, Norway*
[b] *Norwegian College of Fishery Science, University of Tromsø, N-9037 Tromsø, Norway*

Received 4 January 2001; accepted 11 January 2002

**Abstract**

The distribution of chlorophyll-*a* in the Barents Sea was observed from the optical satellite instrument Sea-viewing Wide Field-of-view Sensor (SeaWiFS) during May 1999. In the same period water samples were collected in situ and analysed. Contrary to previous studies of phytoplankton distribution in the Barents Sea, we rigourously analysed the chlorophyll-*a* distribution characteristics with respect to sea ice and oceanographic conditions, spatially and temporally. The spatial distribution of surface chlorophyll-*a* was analysed and related, statistically, to the ice edge and sea ice concentrations from the Special Sensor Microwave Imager (SSM/I) satellite instrument. The highest chlorophyll-*a* concentrations were observed near the ice edge, and then decreased further into the ice. The spatial variability of the chlorophyll-*a* concentrations in this region was high, even in open water along the ice edge. The chlorophyll-*a* observations indicated a strong primary bloom about 2 weeks after the ice edge had retreated from a given measurement point. There were also indications of several minor blooms about 2 weeks after the initial bloom. The vertical distributions of chlorophyll-*a* are presented for nine different stations in the Marginal Ice Zone (MIZ) of the northern Barents Sea and discussed in terms of simultaneously measured temperature–salinity CTD profiles. Water mass properties and sea ice history have a significant impact on the vertical distribution of phytoplankton. The surface chlorophyll-*a* concentration was about 60% higher ($\pm$ 70% S.D.) than the total column average. The correlation coefficient was 0.87, indicating that surface values are good predictors for relative levels of total phytoplankton biomass during spring conditions. We propose a method to identify the stage of the phytoplankton bloom based on satellite observations of chlorophyll-*a*, temperature, salinity and sea ice history. Based on an extensive set of field measurements at different times from many locations in the Barents Sea, we have produced empirical formulae to estimate the integrated chlorophyll-*a* content for the water column from surface (satellite) measurements during early spring (homogeneous water masses) and bloom conditions.


*Keywords:* Phytoplankton; Chlorophyll; Sea ice; CTD observations; Ocean colour; Satellite imagery

## 1. Introduction

Arctic water masses north of the Polar Front are generally less productive than Atlantic water masses, and the production becomes concentrated to the

* Corresponding author. Present address: Norwegian Institute for Air Research, N-9296 Tromsø, Norway. Tel.: +47-777-50375; fax: +47-777-50376.
*E-mail address:* Ola.Engelsen@nilu.no (O. Engelsen).

0924-7963/02/$ - see front matter 
PII: S0924-7963(02)00077-5

vicinity of the ice edge. The well-known ice edge effect (Sakshaug and Skjoldal, 1989; Strass and Nöthig, 1996; Sakshaug, 1997) has a major influence on the spring bloom pattern of chlorophyll-*a* in the Barents Sea. Melt water causes salinity gradients in the water column, thus forming a Surface Mixed Layer (SML) which confines the phytoplankton mainly within the euphotic zone. The SML is the stratified density field above the uppermost pycnocline, defined by a halocline between melt water layers and deeper water masses with higher salinity. This stratification of the upper water masses combined with a generally ample supply of nutrients after the winter, increased radiation from rising solar elevations and decreased sea ice concentrations during the spring, sets the condition for a vigourous phytoplankton production near the surface (Syvertsen, 1991; Melnikov, 1997; Falk-Petersen et al., 1998; Hegseth, 1998). Thus, the onset of plankton blooms is directly related to the seasonal availability of incident light and melting of the ice (Sakshaug and Slagstad, 1991). In contrast, the phytoplankton variability in ice-free

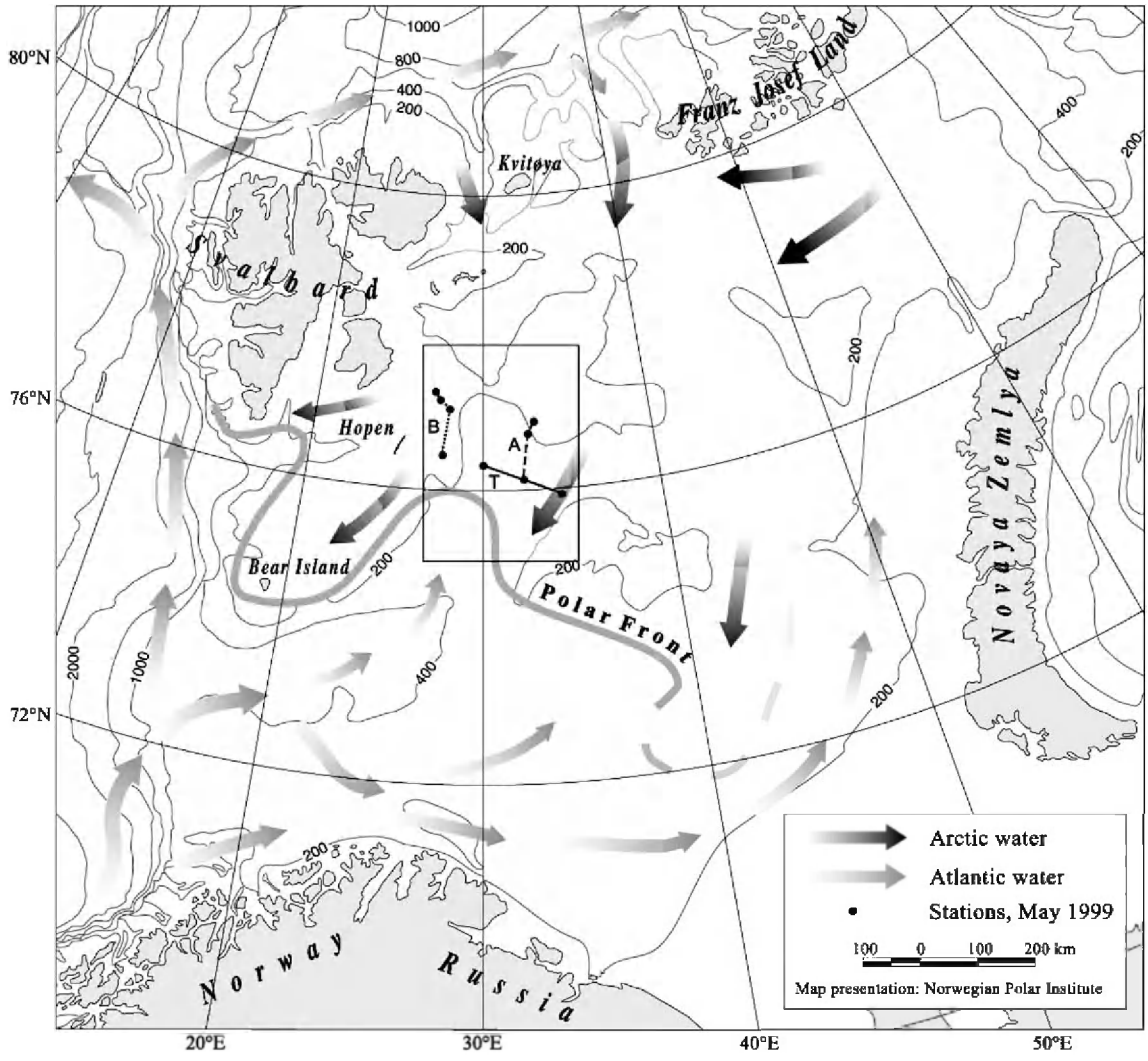


Fig. 1. Map of the Barents Sea. The Polar Front and bathymetry with 200- and 400-m isolines are shown, and the study area is limited by the rectangle.

waters is a function of both light through the water column (Sverdrup, 1953) and nutrient supply from, e.g., vertical mixing (Dutkiewicz et al., 2001).

The peak of the bloom in the Barents Sea may reach biomass (chlorophyll-*a*) values of 20 mg $m^{-3}$ at the surface, and integrated values up to 900 mg $m^{-2}$ for the upper 50 m of the water column (Hegseth, 1992). The magnitude of the annual primary production in the northern Barents Sea is related to spatial variation in ice cover, which is partly determined by the inflow of warm Atlantic water, and stratification of the water column caused by the melting processes. During the seasonal ice melt, algal blooms sweep across the entire northern Barents Sea, and the total annual production is about 40–50 g C $m^{-2}$ (Rey and Loeng, 1985; Wassmann and Slagstad, 1993; Hegseth, 1998).

The seasonally high primary production in the Marginal Ice Zone (MIZ) is the ultimate reason for its great ecological importance. The large production along the ice-edge and far into the ice zone itself results in a high abundance and biomass of temporary and permanent ice-fauna (Lønne and Gulliksen, 1989; Hop et al., 2000) and zooplankton (Falk-Petersen et al., 1999). The strong seasonal pulse of energy through the ice-associated and pelagic marine food webs directly influences the abundance of upper trophic levels, represented by large marine mammal and sea bird populations in and around the northern Barents Sea (e.g., Haug et al., 1994; Wiig, 1995; Anker-Nilsen et al., 2000).

Marginal Ice Zones are some of the most dynamic areas in the world's oceans. The latitudinal location of the ice edge during summer in the Barents Sea can vary by hundreds of kilometres from year to year (Gloersen et al., 1992), and there is a strong correlation between the North Atlantic Oscillation (NAO) winter index and the maximum sea ice extent during spring (Vinje, 2001). The interaction between the atmosphere, ocean and sea ice is strong within the MIZ and adjacent sea, with large variations in ocean–ice–atmosphere heat flux and momentum transfer over short distances (order of a few kilometres). Near the ice edge, mesoscale interactions result in strong hydrodynamic instabilities, producing eddies, jets and

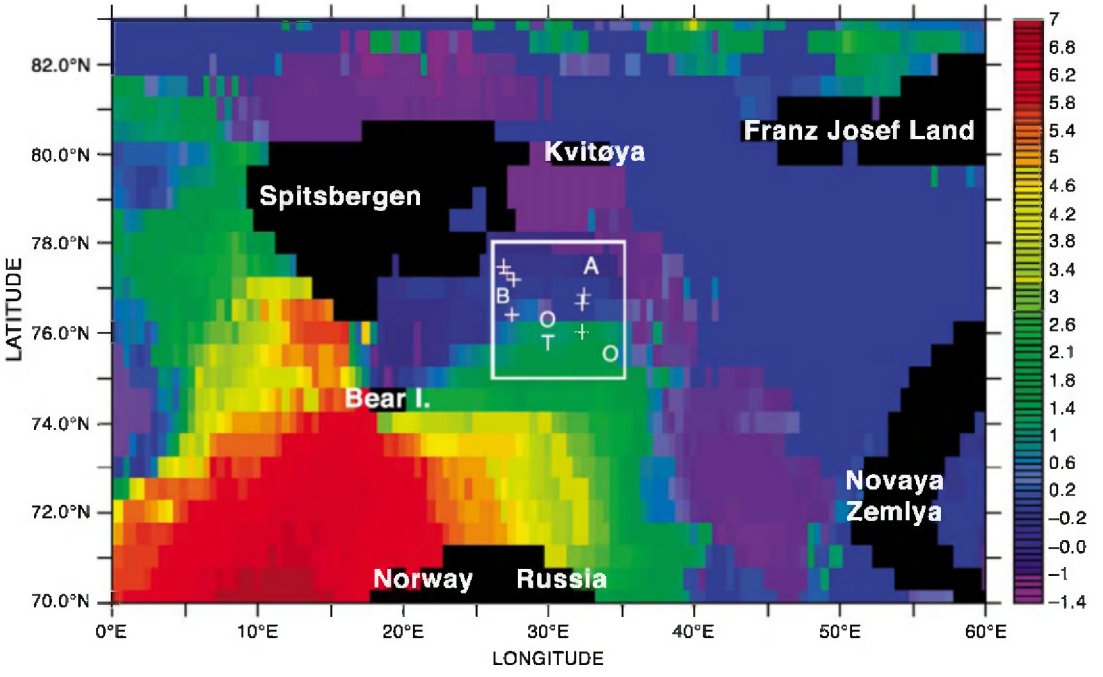


Fig. 2. Sea Surface Temperature (°C) obtained from the NOAA AVHRR sensor. The map is a mosaic with 50-km resolution, shown for 15 May 1999 but using data from adjacent days in a 3–4-days period. Arctic water is shown in blue and Atlantic water is yellow and red, and the Polar Front is located in or near the green area. The SST map has been generated interactively by NOAA Satellite Active Archive (http://las.saa.noaa.gov).

filaments that redistribute ice, heat, salt and momentum over scales of 5–10 km. The ice edge zone may also undergo rapid changes in ice cover extent and concentration because of changing wind directions. Conventional ice–ocean–biological production models cannot accurately represent the highly variable conditions of the Marginal Ice Zone.

The water masses of the northern Barents Sea are characterised by influx of cold Arctic water from the north (Fig. 1). At the Polar Front, the cold Arctic water meets warmer Atlantic water from the North Atlantic current, which subsides below the less saline Arctic water masses. The Polar Front generally follows the bottom topography at 250-m depth (Gawarkiewicz and Plueddemann, 1995), although the approximate location of the front can also be observed as the boundary between warm Atlantic and cold Arctic waters. The maximum ice extent during winter often coincides with the Polar Front (Loeng, 1991). During the late spring period, when our sampling was performed, the ice edge had started to retreat northwards because of melting.

In this paper, we present and compare the distribution of chlorophyll-*a* in the Barents Sea, based on data from both the Sea-viewing Wide Field-of-view Sensor (SeaWiFS) optical satellite instrument and in situ water samples taken during May 1999. Contrary to previous studies of phytoplankton distribution in the Barents Sea, we rigourously analysed the chlorophyll-*a* distribution characteristics with respect to sea ice and oceanographic conditions, both spatially and temporally.

An important motivation was to explore the potential of SeaWiFS satellite measurements. Earlier inves-

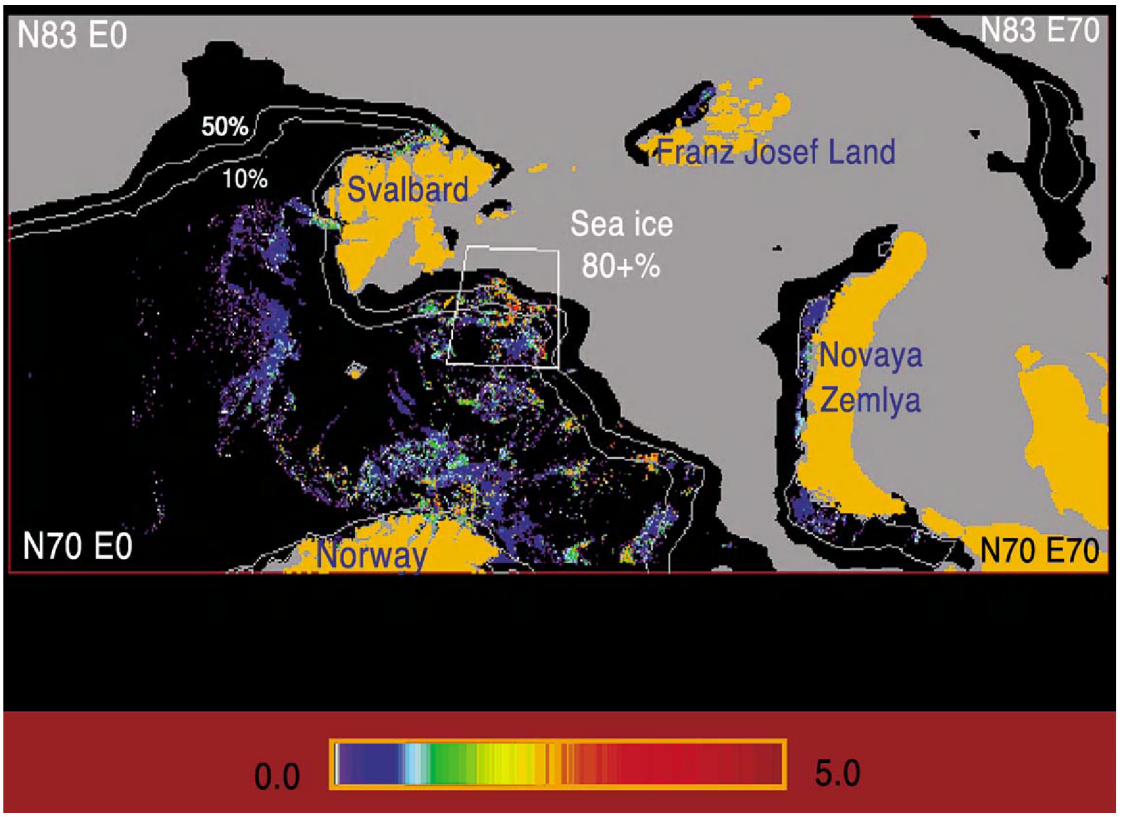


Fig. 3. Colour-coded map of chlorophyll-*a* distribution (mg Chl-*a* $m^{-3}$) in the Marginal Ice Zone of the northern Barents Sea based on SeaWiFS data for the period of 6–21 May 1999. Black areas contain no data due to quality flagging, whereas solid grey is areas with 80% or more sea ice concentrations on 16 May 1999. The two other grey isolines are 10% and 50% sea ice concentrations on this day. The area inside the white frame is shown enlarged in Fig. 4.

tigations in the 1980s with data from the Coastal Zone Color Scanner (CZCS) have only produced composite pictures from the summer period (Kögeler et al., 1995; Kögeler and Rey, 1999). In general, chlorophyll-*a* can be measured more accurately in situ than from space. In fact, most current satellite retrieval algorithms are still to some extent empirically derived based on former in situ measurements (Aiken et al., 1995; Carder et al., 1999; Clark, 1999). In situ data are limited in spatial and temporal coverage, generally to a number of point measurements, whereas satellite recordings have large areal coverage and high revisit rates. Cloud cover masking the sea surface is one of the main limitations for satellite observations (Joint and Groom, 2000).

If satellite information on phytoplankton biomass and/or primary production is to be used on a large scale, phytoplankton must be reliably quantified in terms of sea-surface chlorophyll which can be extended to integrated plankton biomass for the water column (Morel et al., 1996). The relationship between surface chlorophyll-*a* and mean water column concentrations within the euphotic zone (0–50 m) was studied based on our field data from May added by historical data (back to 1986) from the Barents Sea for March through October. The data are discussed in relation to phytoplankton growth phase and equations for calculation of total chlorophyll-*a* from surface values for three different phytoplankton bloom phases.

## 2. Materials and methods

The present study was carried out as a part of two multidisciplinary research programmes: "Ecological and physical processes in the Marginal Ice Zone of the Northern Barents Sea (ICE-BAR)" and "Temporal and spatial variability of the ice–ocean system of the ice-edge in the Marginal Ice Zone of the Barents Sea" headed by the Norwegian Polar Institute. In situ data were collected during a cruise with R/V 'Lance'

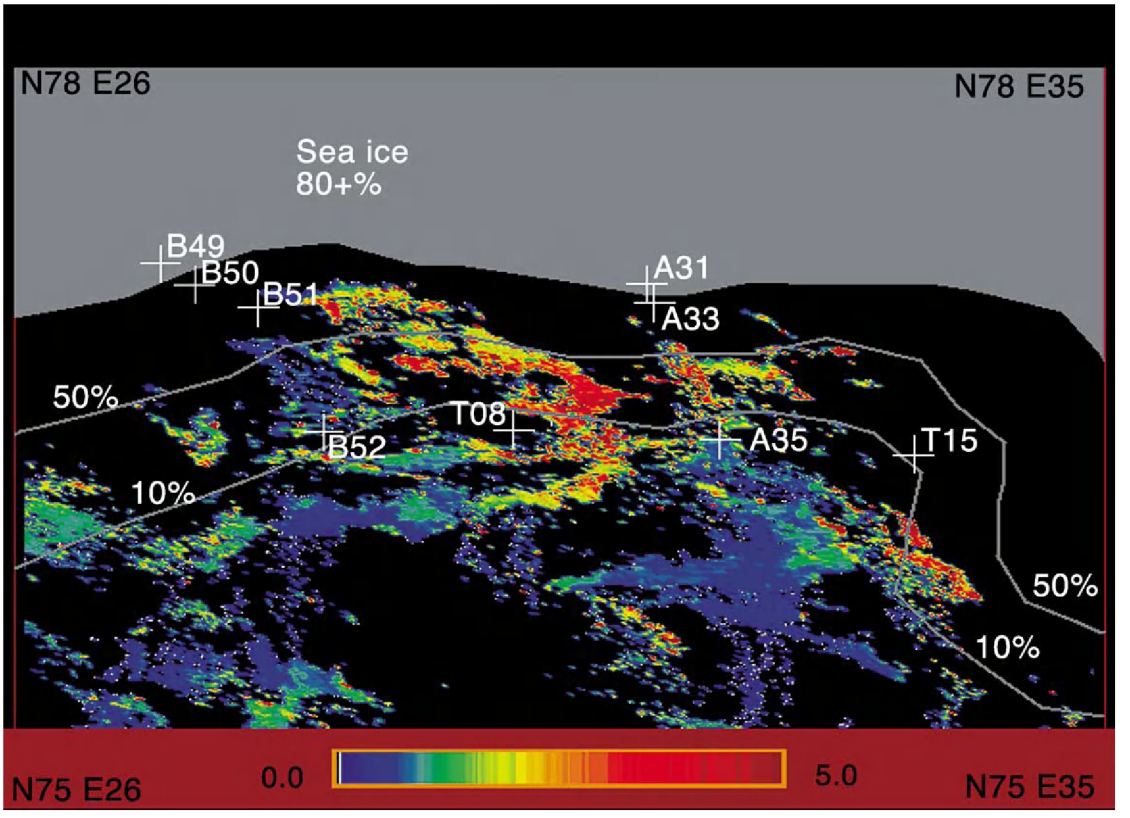


Fig. 4. A more detailed chlorophyll-*a* distribution, extracted from Fig. 3.

during 5–24 May 1999. The cruise consisted of one transect (T) along the ice edge from 26–34°E (5–7 May), and two transects into the Marginal Ice Zone at about 33°E (8–15 May) in the central Barents Sea (transect A) and at about 27°E (16–24 May) near the Hopen Island (transect B). A total of nine stations were allocated at different locations on these transects in the Marginal Ice Zone (Figs. 2, 4). Throughout this paper, each station is referenced with a transect ID (A, B or T) followed by a station ID (08-52).

The vertical distribution of chlorophyll-*a* was determined at each station. Eight chlorophyll-*a* samples were collected with a Niskin bottle mounted on a CTD sonde, from discrete depths ranging from 0 to 100 m. The chlorophyll-*a* in the water samples was determined fluorometrically. Seawater samples (50 ml) were filtered, in parallels, onto GF/F filters and frozen onboard. The samples were analysed in Tromsø after the cruise using methanol as extracting agent (Holm-Hansen and Riemann, 1978).

Water mass properties (i.e., temperature and salinity) were recorded at each station with a Sea-Bird

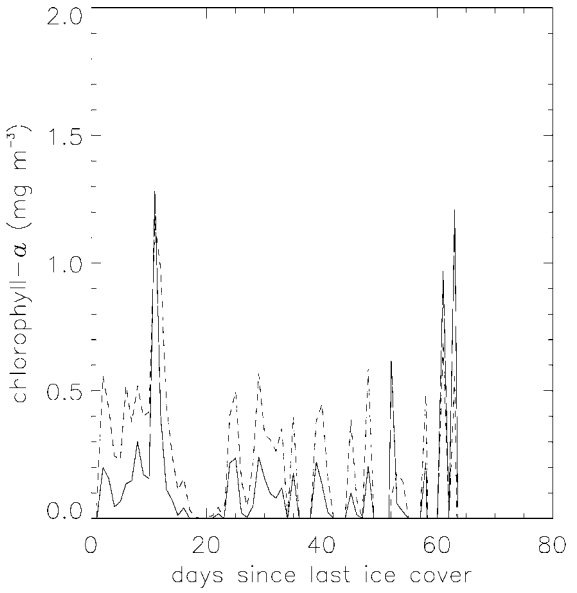


Fig. 5. SeaWiFS chlorophyll-*a* data from the Barents Sea, in the period of 6–21 May 1999, with respect to ice cover history. The mean (solid line) with standard deviation (dashed line) of each group of chlorophyll-*a* values indicates the general relationship between chlorophyll-*a* and the duration of reduced ice concentration (< 50%). Note that zero chlorophyll-*a* in this case means that no data were available.

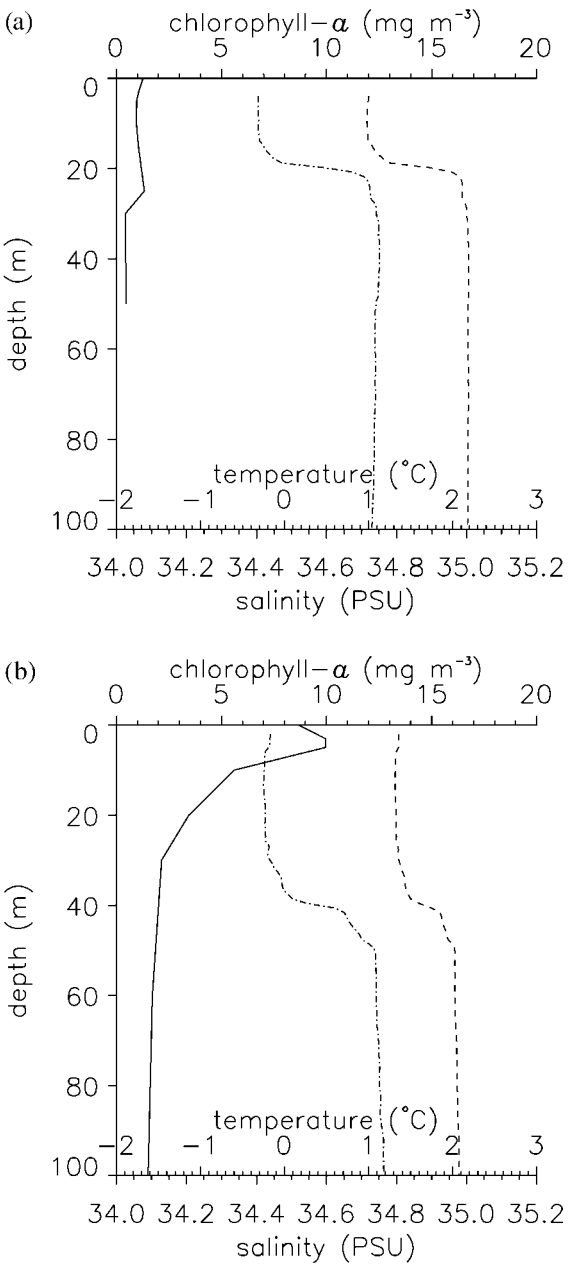


Fig. 6. Chlorophyll-*a* and CTD stations in open water near the ice edge, for transect T. Solid: chlorophyll-*a* (mg Chl-*a* $m^{-3}$); dashed: Salinity (PSU); dash-dot: Temperature (°C). (a) Station T08: N76°20.7′ E30°00′ . Date: 6 May 1999, western station. (b) Station T15: N75°52.2′ E34°24.5′ . Date: 7 May 1999, eastern station.

Electronics SBE 911+CTD (Conductivity–Temperature–Density) sonde deployed vertically from R/V 'Lance'. The sonde yielded temperature and salinity ($T$–$S$) measurements at increments of 1 dbar water pressure from the surface down to the sea floor.

Sea Surface Temperatures (SST) can now be obtained operationally from a number of infrared satellite sensors. For convenience, we obtained pre-processed data from the NOAA Satellite Active Archive based on the Advanced Very High Resolution Radiometer (AVHRR) with 1.1-km resolution. However, the spatial resolution has been downgraded from 1.1 to 50 km in the mosaic processing. The SST map is generated twice weekly by integrating SST observations obtained during the period since the last analysis (NOAA KLM user's guide, http://www2.ncdc.noaa.gov/docs/klm/html/c9/sec9-1.htm).

Sea ice concentrations originate from Special Sensor Microwave Imager (SSM/I) data. They were provided by the Earth Observation System (EOS) Distributed Active Archive Centre (DAAC) at the National Snow and Ice Data Center, 1995, University of Colorado, USA. The SSM/I instrument is mounted on the Defence Meteorological Satellite Program (DMSP) F-13 satellite, and is a passive microwave radiometer with a spatial resolution of 25 km. The NASA Team Algorithm (Cavalieri et al., 1997) was used in the computation of mean sea ice concentrations from daily brightness temperatures. By collecting a time series of SSM/I data from the Barents Sea, the history of the total ice concentrations of each station for a period of 2–3 months before the cruise was derived.

The distribution of chlorophyll-*a* was observed from the SeaWiFS optical satellite instrument at spatial resolutions down to 1.1 km. Due to the physical constraints of the imaging process, the SeaWiFS data mainly represent the chlorophyll-*a* content near the ocean surface (e.g., Mobley, 1994). The SeaWiFS chlorophyll-*a* data were derived from LAC level 1A data (i.e., radiances at the top of the atmosphere), using the SeaDAS software package version 3.3 (http://seadas.gsfc.nasa.gov). All data pertain to version 2 of the calibration and processing facility. Up to four daily scenes were available for the Barents Sea throughout the cruise. All pixels that were flagged for erroneous data (e.g., under cloudy conditions), were discarded. The remaining pixels were geo-referenced into a 1-km grid. When more than one chlorophyll-*a* value was available for a given position, the measurement closest in time to 14 May 1999 (i.e., the middle of the period for data collection) was selected. However, whenever more than one daily satellite measurement was available, priority was always given to data taken at the highest possible solar elevation. The SeaWiFS data were re-projected to be superimposed with the sea ice and oceanographic data in an isotropic Lambert's azimuthal equal-area projection.

For each "good pixel" of chlorophyll-*a* from the SeaWiFS sensor, we counted the number of days of ice-free conditions at its location before the time of the satellite measurement. All chlorophyll-*a* values were then grouped according to the number of days since their sampling location was covered by sea ice. The ice cover history was derived from the daily total sea ice concentrations available from the SSM/I data, with 50% total ice concentration defined as the upper cut-off point for ice-free conditions in this particular case.

## 3. Results

Below we join observations of oceanic chlorophyll-*a*, temperature, salinity, and sea ice concentrations in order to analyse how they interrelate.

Sea Surface Temperatures, determined by the AVHRR satellite sensor, shows that the Arctic

Table 1
Chlorophyll-*a* at the surface ($S$) (mg Chl-*a* $m^{-3}$) and integrated values ($F$) (mg Chl-*a* $m^{-2}$) for the upper 50 m of the water column in the northern Barents Sea, May 1999

| Date (1999) | Station no. | $S$ = Surface (mg Chl-*a* $m^{-3}$) | $F$ = Integrated 0–50 m (mg Chl-*a* $m^{-2}$) | 50 $S/F$ |
|---|---|---|---|---|
| 6 May | T08 | 1.26 | 32.48 | 1.94 |
| 7 May | T15 | 8.67 | 195.29 | 2.21 |
| 9 May | A31 | 3.34 | 162.14 | 1.03 |
| 11 May | A33 | 12.70 | 286.62 | 2.21 |
| 13 May | A35 | 7.71 | 293.91 | 1.31 |
| 17 May | B49 | 1.42 | 30.44 | 2.34 |
| 18 May | B50 | 0.31 | 68.22 | 0.23 |
| 19 May | B51 | 5.58 | 158.22 | 1.77 |
| 21 May | B52 | 6.79 | 280.36 | 1.21 |
| Mean | | 5.309 | 167.52 | 1.583 |

The mean water column chlorophyll-*a* concentration is $I = F/50$. The ratio of surface-to-integrated values indicates the relative magnitude of the surface phytoplankton bloom. See Fig. 4 for station locations.

surface water (shown in blue) has a temperature below 0 °C (Fig. 2). Atlantic surface water (red/yellow) holds more than 2 °C when reaching the Polar Front (green). The study site was located in the vicinity of the Polar Front (Figs. 1 and 2).

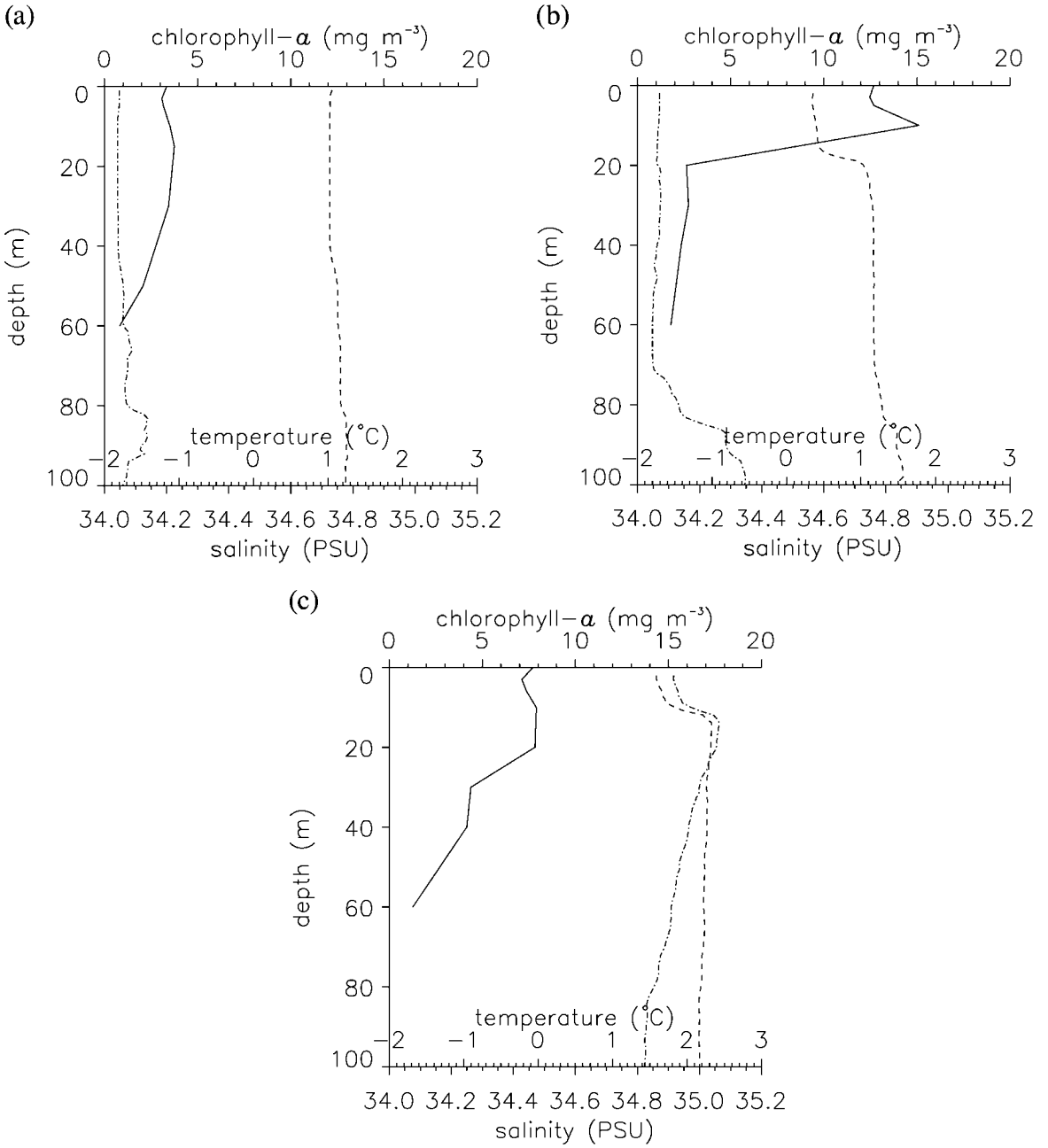


Fig. 7. Same as Fig. 6, except that chlorophyll-*a* and CTD stations are inside the Marginal Ice Zone at eastern transect A. (a) Station A31: N76°57.8′ E32° 59.8′ Date: 9 May 1999, furthermost into the ice. (b) Station A33: N76°48.9′ E32°49.2′ Date: 11 May 1999, inside the MIZ. (c) Station A35: N76°07.7′ E32°20.0′ Date: 14 May 1999, near open water.

The chlorophyll-*a* distribution for the Barents Sea shows a belt of high phytoplankton biomass near the ice edge (Fig. 3). A more detailed image from this area (Fig. 4) shows that the surface chlorophyll-*a* concentration may change 10-fold over a distance of a few kilometres. This confirms that the spatial

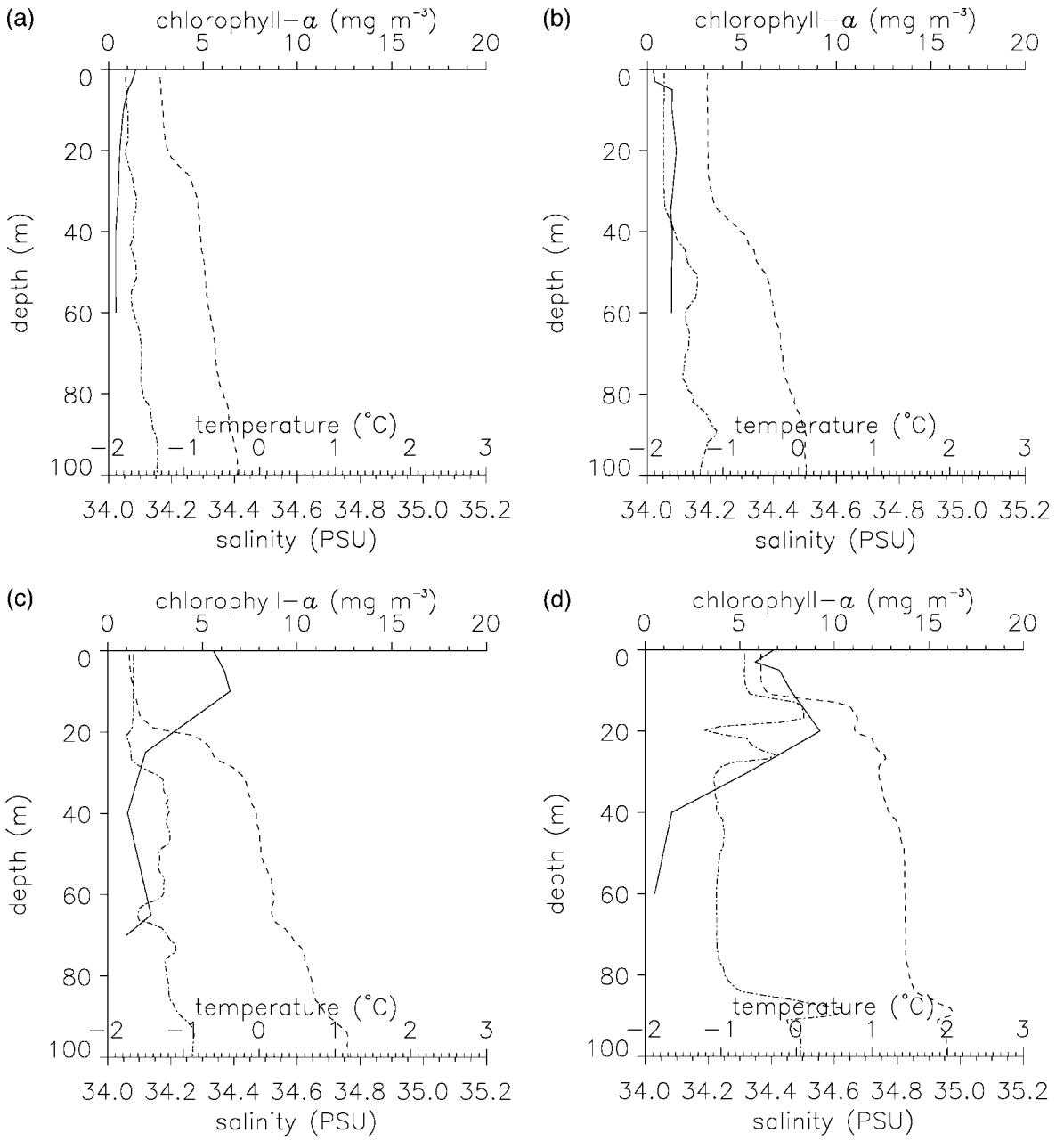


Fig. 8. Same as Fig. 7, except that this is further west at western transect B. (a) Station B49: N77°25.6′ E27°01.0′ Date: 17 May 1999, furthermost into the ice. (b) Station B50: N77°18.0′ E27°16.8′ Date: 18 May 1999, inside the MIZ. (c) Station B51: N77°08.4′ E27°54.9′ Date: 19 May 1999, inside the MIZ. (d) Station B52: N76°29.6′ E27°42.7′ Date: 21 May 1999, near open water.

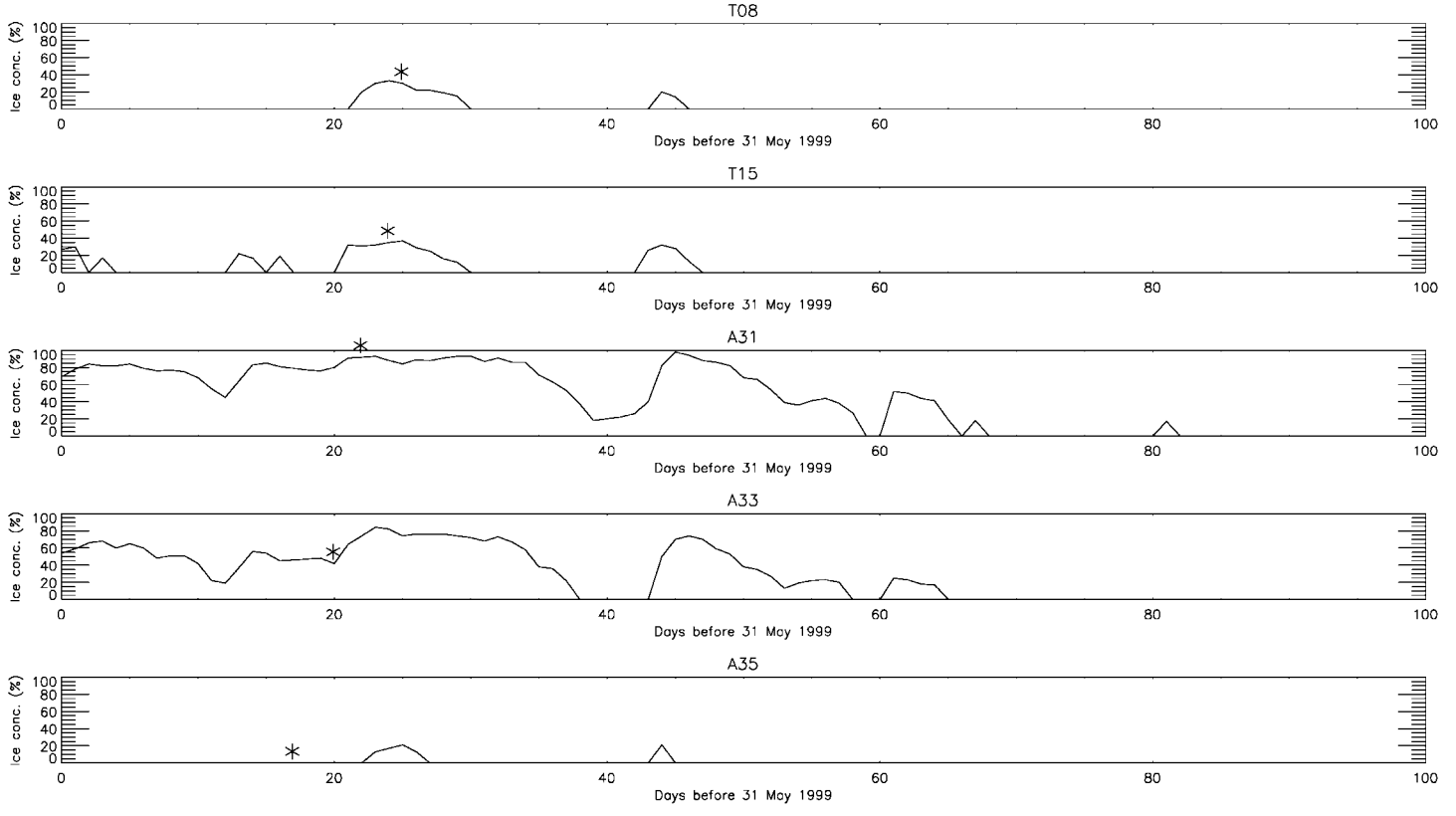


Fig. 9. Total ice concentration history for each of the stations. The star (*) on each plot indicates the actual time of measurements.

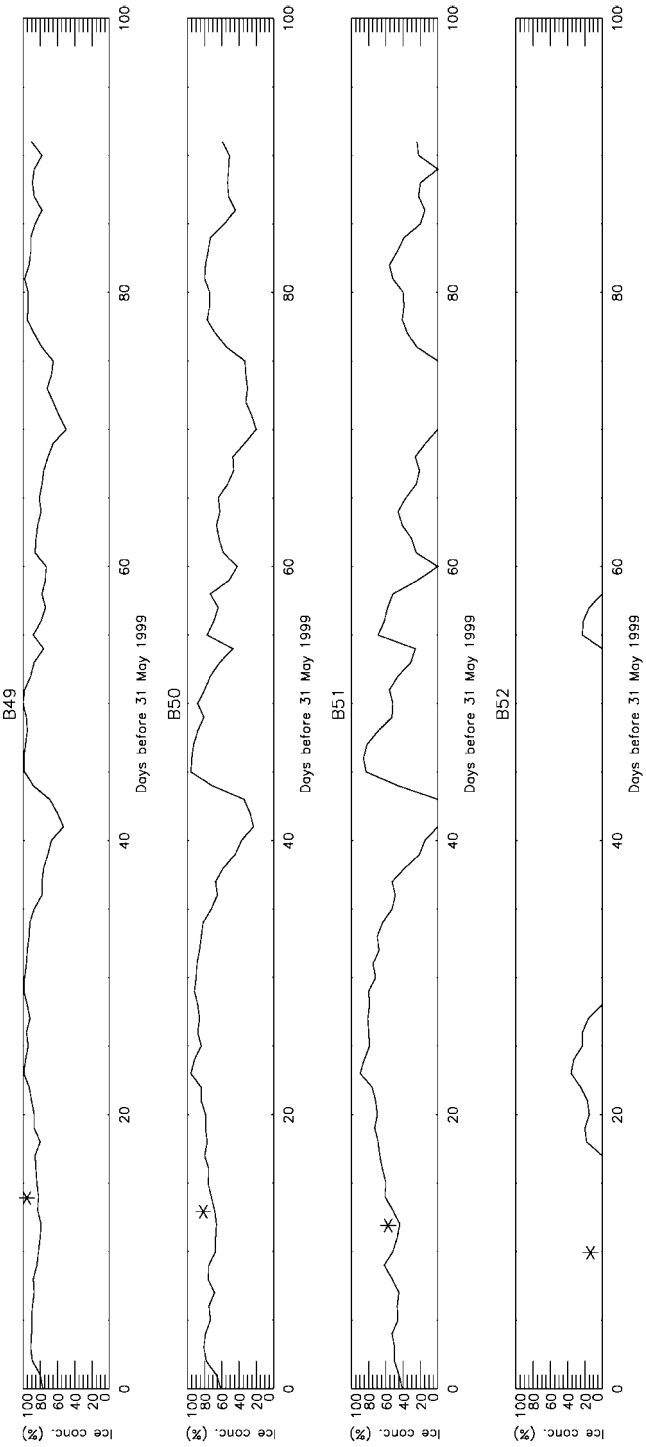


Fig. 9 (*continued*).

variability of phytoplankton biomass is extremely high in the Marginal Ice Zone.

The magnitude of chlorophyll-*a* in the Barents Sea, as observed from SeaWiFS, is strongly related to the duration of ice-free waters at each point of observation (Fig. 5). The temporal dynamics in this graph is very large, but shows that blooms develop only after a period of open water in the area. The position and movements of the ice edge thus have a significant impact on phytoplankton concentrations. The chlorophyll-*a* observations from SeaWiFS in relation to sea ice history indicated a strong phytoplankton bloom about 2 weeks after the ice edge had receded from a given measurement point. We also observed indications of several minor blooms after the initial bloom. It was anticipated that the dispersion of the major bloom peak in both time and magnitude, and the existence of minor peaks, might be caused partly by movements of the sea ice edge as well as variations in ice concentrations because of wind and currents. Also note that the SeaWiFS only measures the surface concentration. Fluctuations in water mass properties may alter the vertical profile of chlorophyll-*a* and thus influence the satellite observations.

Vertical profiles of chlorophyll-*a* and simultaneous values for salinity and temperature were determined for the three different transects including the nine stations (Figs. 6–8). Phytoplankton blooms were recorded in different stages; pre-bloom, bloom and late bloom. In the bloom stage the phytoplankton biomass is concentrated near the surface, but it starts to sink in a late bloom, and eventually a deep chlorophyll-*a* maximum can be observed.

### 3.1. Pre-bloom

At an early station near the outer ice edge (T08, Fig. 6), the water masses were stratified, but the algal bloom had barely commenced. The small phytoplankton biomass present was spread evenly throughout the Surface Mixed Layer (SML), extending to 20-m depth. The chlorophyll-*a* was slightly elevated in this layer but still only 1.3 mg Chl-*a* $m^{-3}$ (Table 1). The ice concentration at this station was increasing (Fig. 9) because of advected ice from the north, which may have resulted in decreased algal growth because of the consequent decline in light. Western stations that were far into the ice (B49 and B50, Fig. 8) had more than 8 days of decreasing ice densities, but concentrations were still more than 70%. At such high ice concentrations, the SML had not become well established, and the phytoplankton biomass was correspondingly low.

### 3.2. Bloom

With the onset of melting and subsequent stratification, conditions became optimal for phytoplankton growth, and the typical vertical profile of algal blooms at the ice edge appeared, as seen at, e.g., station T15 (Fig. 6). At this station in the outer ice edge, the algal bloom was well developed with surface chlorophyll-*a* values in the range of 8–10 mg Chl-*a* $m^{-3}$. The SML was deeper, approximately 40 m, and the phytoplankton bloom was confined to this layer, with a maximum near the surface. Compared to T08, this station had 1–2 days of decreasing ice concentration. The melting process had lasted longer at station T15 and the bloom had been given more time to develop. The maximum chlorophyll-*a* observed in our SeaWiFS data was 16 mg $m^{-3}$ (this value is not shown in our figures). It was recorded after 22 days of low ice concentration (50% or less).

Another station at outer part of the ice zone (A33, Fig. 7) was also in bloom phase, with maximum concentration of 15 mg Chl-*a* $m^{-3}$. This station had experienced a rapid decline in ice concentration from 85% to 40% in less than 3 days, which resulted in more available light at the surface. The ice cover could have been reduced by wind forcing or melting; the latter would have contributed to the formation of an SML. In either way, the improved light conditions triggered a strong bloom.

At the eastern station furthest into the ice zone (A31, Fig. 7), the ice concentration had also decreased, but only for 1–2 days (as for station T15). Although the ice was very dense (90%), there seemed to be enough light to sustain a substantial phytoplankton biomass. We are unsure whether an SML of 50-m depth exists in this case. The sea water densities at 40 and 60 m only differed by 0.0191 kg $m^{-3}$. A considerable proportion of the chlorophyll-*a* was found in deeper waters, with chlorophyll-*a* maxima of 8–9 mg Chl-*a* $m^{-3}$. The CTD observations at station A31 resembled a typical winter condition with well-mixed water masses.

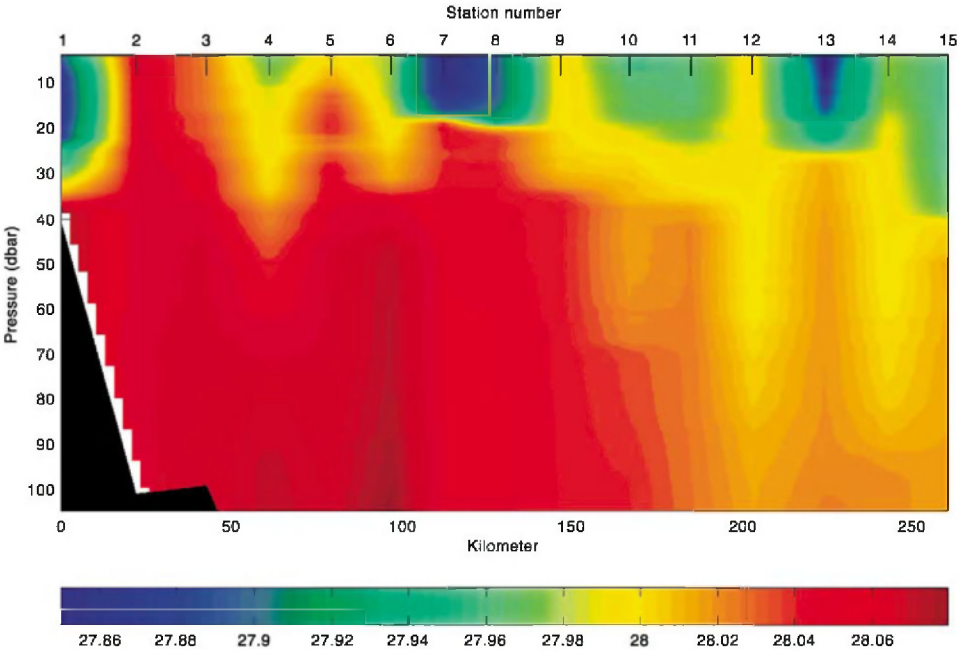


Fig. 10. Mass densities − 1000 (kg $m^{-3}$) of water masses in an approximately linear transect along the ice edge (about 10% ice concentration) on an extended transect T starting from N76.58°E 25.80° (T01) to N75.87° E34.41° (T15). Exact measurements were done for each station, whereas intermediate values are interpolated.

### 3.3. Late bloom

One station near the outer part of the ice zone (B51, Fig. 8) seemed to be in a late bloom stage, where the plankton populations were in the process of sinking. Similarly to station A33, it had experienced a rapid decline of ice concentrations from 85% to 40% over a short time, although the growth conditions may have been better here for a longer period of time.

The stations located in open water (A35 and B52, Figs. 7 and 8) had similar ice histories as the stations near the ice edge (T08 and T15), but had been ice-free (i.e., 0% ice concentration) for 5 or more days. The phytoplankton bloom had been progressing for some time, and those stations had reached a late bloom stage where the chlorophyll-*a* vertical profiles showed a characteristic deep maximum near the pycnocline, indicating sinking phytoplankton populations. The

Table 2
Relationships between surface chlorophyll-*a* concentrations ($S$) (mg Chl-*a* $m^{-3}$) and mean chlorophyll concentrations ($I$) (mg Chl-*a* $m^{-3}$) in the water column down to 50 m measured at different times of the year in the Barents Sea, both in open and ice covered waters

| Season | Growth phase | $n$ | $a$ | $b$ | $r^2$ | $x$ | SD |
|---|---|---|---|---|---|---|---|
| March–July | No bloom, homogeneous water masses | 14 | 1.008 | − 0.024 | 0.997 | 1.04 | 0.07 |
| March–October | Pre-bloom and bloom phase | 41 | 0.944 | 0.230 | 0.978 | 1.78 | 0.63 |
| May–October | Post-bloom, with deep chlorophyll maximum | 22 | 0.378 | 0.153 | 0.336 | 0.47 | 0.31 |
| March–October | All data | 77 | 0.706 | − 0.063 | 0.654 | 1.27 | 0.76 |

Data are grouped into three different conditions: homogeneous water masses, pre-bloom/bloom phase and post-bloom phase. The log-linear equation, $\log I = a \log S + b$, expresses the relationship between surface and water column chlorophyll-*a*. In the table, $n$ is the number of observations for each calculation, $a$ and $b$ are equation parameters, $r^2$ is the correlation coefficient, and $x$ is the mean ratio between surface and mean water column chlorophyll-*a* concentrations, including the standard deviation (SD).

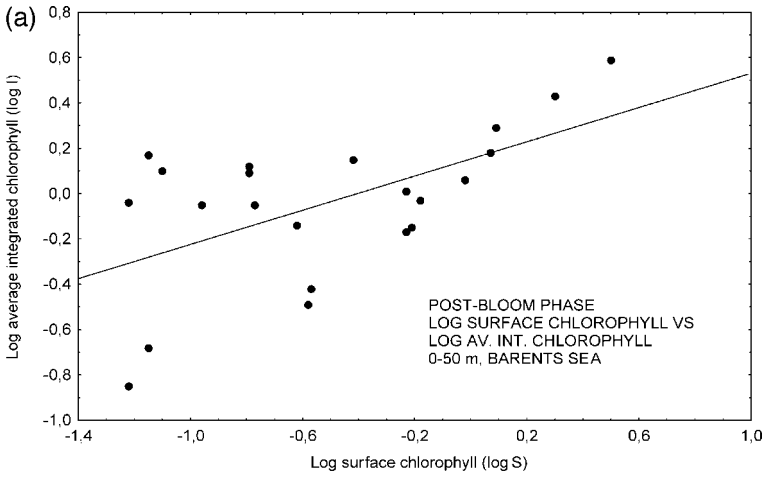
(a)
Log average integrated chlorophyll (log I)
0,8
0,6
0,4
0,2
0,0
-0,2
-0,4
-0,6
-0,8
-1,0
-1,4
-1,0
-0,6
-0,2
0,2
0,6
1,0
Log surface chlorophyll (log S)
POST-BLOOM PHASE
LOG SURFACE CHLOROPHYLL VS
LOG AV. INT. CHLOROPHYLL
0-50 m, BARENTS SEA

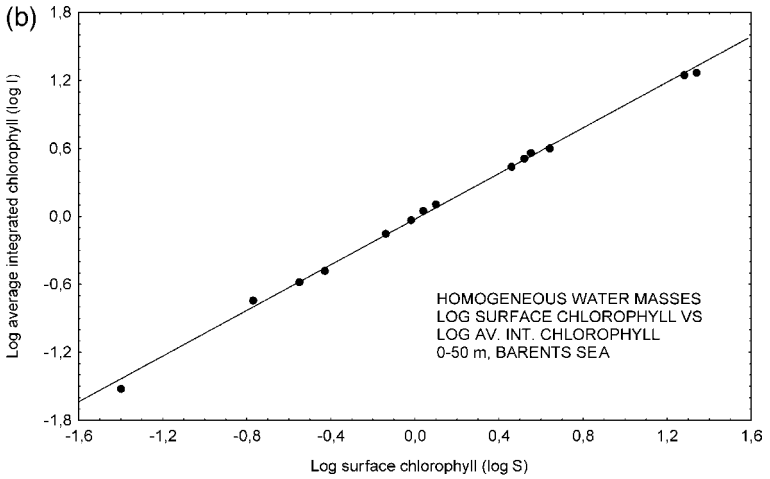
(b)
Log average integrated chlorophyll (log I)
1,8
1,2
0,6
0,0
-0,6
-1,2
-1,8
-1,6
-1,2
-0,8
-0,4
0,0
0,4
0,8
1,2
1,6
Log surface chlorophyll (log S)
HOMOGENEOUS WATER MASSES
LOG SURFACE CHLOROPHYLL VS
LOG AV. INT. CHLOROPHYLL
0-50 m, BARENTS SEA

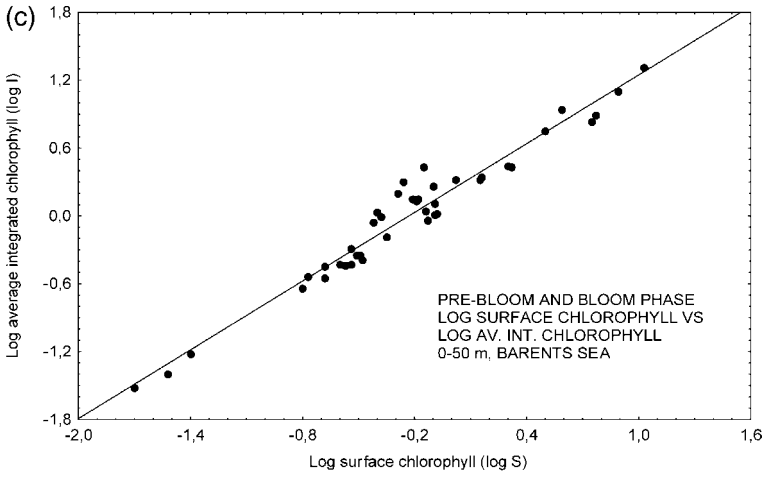
(c)
Log average integrated chlorophyll (log I)
1,8
1,2
0,6
0,0
-0,6
-1,2
-1,8
-2,0
-1,4
-0,8
-0,2
0,4
1,0
1,6
Log surface chlorophyll (log S)
PRE-BLOOM AND BLOOM PHASE
LOG SURFACE CHLOROPHYLL VS
LOG AV. INT. CHLOROPHYLL
0-50 m, BARENTS SEA

open water stations were thus approaching a post-bloom phase.

The history of total ice concentration for each station provided additional background information, which may help explain the shape of their chlorophyll-*a* profiles (Fig. 9). Stations T08, T15, A35 and B52, all located near the ice edge or in open water, had essentially the same ice history, except that their time of measurements were shifted. Their positions had generally been ice-free (i.e., 0% ice concentration), except for a 10-day period during or just before the measurements. Station T08 had increasing ice concentration, whereas Station T15 was in a state of decreasing ice density. Stations A35 and B52, located near open water, had been completely ice-free for at least 5 days. The ice concentrations at the stations inside the ice zone had all decreased over time before the chlorophyll-*a* sampling, but at different rates and for different lengths of time. Their ice concentrations varied from 90% (A31) to 40% (B51).

The spatial variability found in our SeaWiFS chlorophyll-*a* agrees with that of the water masses measured during our cruise transects along the ice edge (Fig. 10). Sharp boundaries only a few kilometres apart can exist between unstratified water masses with pre-bloom conditions and waters with well-developed SMLs where strong phytoplankton blooms may occur.

In order to estimate the absolute value of total phytoplankton biomass from surface chlorophyll-*a* observations, assumptions on the overall vertical chlorophyll-*a* distribution must be made. The simplest approach is to use surface values as a relative measure of total biomass. The mean ratio between surface chlorophyll-*a* values, measured in situ at nine stations during our cruise, and corresponding mean concentrations for the 0–50-m water column was 1.59 ($\pm$ 0.70 S.D.) (Table 1). The correlation between the surface and water column values was good ($r^2 = 0.87$).

In order to reduce the uncertainty of our results based on a limited data-set, we also considered historical data from Marginal Ice Zone in the Barents Sea (Hegseth, 1992, 1997; Falk-Petersen et al., 1999, 2000). Good correlations between surface and mean water column chlorophyll-*a* concentrations were found for homogeneous water masses and bloom phases, whereas summer conditions with a deep chlorophyll-*a* maximum (post-bloom) yielded an uncorrelated relationship. The ratio between surface and mean water column Chl-*a* concentrations for the bloom phase was on average 1.78, for homogeneous waters it was 1.04, and for post-blooms it was as low as 0.47 (Table 2). For all the Barents Sea data, we found a moderate correlation coefficient ($r^2 = 0.65$). However, fitting the linear equation, $\log I = a \log S + b$, to all available Barents Sea data (Table 2) and then applying summer (i.e., post-bloom phase) surface measurements to this equation, did underestimate total biomass (Fig. 11). This may be expected, because the bulk of phytoplankton biomass is below the surface for the post-bloom scenario.

Although no SeaWiFS observations of chlorophyll-*a* were available for exactly the same location and time as our in situ observations, comparisons with mosaic map pixels, indicated lower observed values from space. The spatial variability of chlorophyll-*a* was large, and the deviations found may not explicitly indicate consistent errors.

## 4. Discussion

The spatial variability of the chlorophyll-*a* concentrations in the MIZ was high, even in open water along the ice edge. The highest chlorophyll-*a* concentrations were observed near the ice edge, and then decreased further into the ice. The chlorophyll-*a* observations indicated a strong primary bloom about 2 weeks after the ice edge (i.e., 50% ice concentration) had retreated from a given measurement point.

Our data have shown that it is possible to predict the phytoplankton biomass in the water column from surface chlorophyll-*a* when the physical factors (i.e., light) are in control of the phytoplankton growth. In such situations, the exponential attenuation of the photosynthetic active radiation (PAR) structures the

Fig. 11. Relationships between log surface chlorophyll-*a* concentrations (mg Chl-*a* $m^{-3}$, log*S*) and log mean chlorophyll-*a* concentrations (mg Chl-*a* $m^{-3}$, log*I*) in the water column down to 50 m measured at different times of the year in the Barents Sea, both in open and ice covered waters. Data are grouped into three different conditions: homogeneous water masses, pre-bloom/bloom phase and post-bloom phase. The least squares linear regression lines are drawn, and their parameters are listed in Table 2.

phytoplankton distribution in the euphotic zone so that the biomass maximum will be found in the surface layers. The correlation between surface and mean water column chlorophyll-*a* concentrations in the SML was remarkably good for bloom conditions, based on our empirical formulae with an extensive background data set. Similar studies of pooled seasonal data from Antarctica also reports good correlations between surface values and total phytoplankton biomass (Holm-Hansen and Mitchell, 1991; Smith et al., 1996; Moline and Prezelin, 2000). When other factors such as nutrient limitation and/or grazing exert control of the deeper phytoplankton growth, there is no longer any predictable correlation between surface and water column phytoplankton biomass. Consequently, only during early spring (homogeneous and pre-bloom) and bloom conditions can total chlorophyll-*a* biomass be derived from surface measurements by satellite. Estimates of total phytoplankton biomass based on satellite data require depth-dependent values of chlorophyll-*a* concentrations (Sathyendranath et al., 1995). Such data can only, with any degree of reliability, be obtained from bloom conditions with a surface biomass maximum or from homogeneous water masses, and probably only apply to the ocean region where they were derived (Joint and Groom, 2000).

Statistical comparisons between surface and mean water column concentrations of phytoplankton indicate that it is useful to devise a method for detecting the various stages of phytoplankton blooms. It would be particularly useful to identify post-bloom conditions when surface measurements of chlorophyll-*a* provide little information on total biomass. Our results indicated that bloom conditions may be separated by jointly analysing environmental parameters such as chlorophyll-*a*, time series of sea ice concentration, sea temperature and salinity. Based on a subset of our own in situ and satellite data, we have indicated the general relationships between bloom stages in terms of approximate ranges and gradients of surface chlorophyll-*a*, SST, surface salinity and ice concentration values (Table 3). Examples of satellite instruments that measure these parameters are in Appendix A. The tabular entries are somewhat speculative since absolute thresholds and gradients for these variables were difficult to quantify with our limited data set. Considering pre-bloom scenarios (T08, B49 and B50, Figs. 6, 8 and 9), we would expect that the ice concentration threshold for a characteristic bloom to be triggered, would be between 40% and 70% during spring conditions in the northern Barents Sea. Using a late bloom scenario (B52, Figs. 8d and 9) as reference, we expect that a post-bloom would involve ice-free conditions for at least 8 days, as well as a low surface chlorophyll-*a* concentration (i.e., less than 1 mg Chl-*a* $m^{-3}$). For homogeneous water masses, with a pre-bloom scenario, we would expect the SST to be near freezing ($-1.8$ °C) and the Sea Surface Salinity (SSS) close to that of Arctic or Atlantic water masses. Bloom and post-bloom scenarios may be characterised by an SST above freezing and rising water temperatures as the melting proceeds. When an SML is established, the SSS is obviously lower than the salinity of the underlying water masses. Neglecting the influence of wind and currents, a time series of SSS observations may detect the formation of an SML. Of course, blooms may be identified by rapid increases of surface chlorophyll, whereas late bloom and post-bloom scenarios have decreasing surface concentrations because the phytoplankton population sinks and plankton growth at the surface become limited by nutrient depletion.

The water and sea ice conditions at which the transition between the different phytoplankton growth phases occur, may depend on the intensity of incoming light. The incoming light, in turn, is heavily influenced by cloud and fog, which are inherent properties of the

Table 3
Approximate levels and gradients ($\Delta$) of sea ice concentration, surface temperature (SST), sea surface salinity (SSS) and chlorophyll-*a* for different bloom stages in the Marginal Ice Zone of the northern Barents Sea

| Growth phase | Ice concentration/$\Delta$ (%) | SST/$\Delta$ (°C) | SSS/$\Delta$ (PSU) | Chl-*a*/$\Delta$ (mg $m^{-3}$) |
|---|---|---|---|---|
| Homogeneous water masses | [0, 100]/+ | < −1.6/0 | > 34.1/0 | < 4/0 |
| Pre-bloom/bloom/late bloom | [0, 70]/− | > −1.8/+ | < 35.0/− | >2/+ |
| Post-bloom | 0/0 | > −1.8/0, + | < 35.0/0,− | < 1/− |

lower atmosphere above the Barents Sea during spring and summer (Vowinkel and Orvig, 1970). Incoming light on a cloudy/foggy summer's day is on average $18 \pm 6\%$ of that of a sunny day, and sunny/partly cloudy days average $55 \pm 20\%$ (Sakshaug and Slagstad, 1991). For example, the average total cloud cover for station T08 was approximately 70% for March and 90% for April and May 1999 (AVHRR Pathfinder producthttp://las.saa.noaa.gov). More data from a large set of representative atmospheric conditions for the Barents Sea should be considered in the future to validate our assumptions. The solar zenith angles at local noon during our cruise in May were $57-61°$.

Most satellite-derived biomass and production estimates have been performed in open waters at low and mid latitudes (e.g., Morel et al., 1996; Joint and Groom, 2000), and few data exist from seasonally ice-covered areas. Our work is a first approach to include the effect of a variable ice cover into satellite observations of chlorophyll-*a* in Arctic waters.

## 5. Conclusions

The spatial variability of the chlorophyll-*a* concentrations in the MIZ is high, both in open water and in ice covered areas. As expected, we observed from SeaWiFS the highest chlorophyll-*a* concentrations near the ice edge in open water, which is typical for ice edge blooms (Rey and Loeng, 1985; Strass and Nöthig, 1996; Sakshaug, 1997).

Phytoplankton blooms can occur from early spring to late autumn in the Barents Sea when sufficient light is available (Hegseth, 1992, 1997, 1998), but our results indicate that a large bloom is most likely to occur about 2 weeks after the ice edge has receded from a given area. Phytoplankton blooms were recorded in different stages; pre-bloom, bloom and late bloom. The progress of phytoplankton blooms is highly dependent on the stratification of the water masses. Using surface chlorophyll-*a*, ice concentration, ice concentration history, Sea Surface Temperature and ocean surface salinity, which can all be derived from satellite data, we have proposed an approach to identify water mass characteristics typical for homogeneous water column, bloom and post-bloom phases. Good correlations between surface and mean water column chlorophyll-*a* concentrations were found for the homogeneous and bloom phases, whereas summer conditions with a deep chlorophyll-*a* maximum (post-bloom) yielded an uncorrelated relationship. Post-bloom conditions may arise in waters that have been ice-free for minimum 8 days. Except for homogeneous (unstratified) water masses, the deviation of surface values of chlorophyll-*a* from mean water column concentrations was substantial.

## Acknowledgements

We thank Józef Wiktor for participation in the collections of water samples.

We would also like to thank the SeaWiFS Project (Code 970.2) and the Distributed Active Archive Center (Code 902) at the Goddard Space Flight Center, Greenbelt, MD 20771, for the production and distribution of LAC level 1A data, respectively. These activities are sponsored by NASA's Mission to Planet Earth Program. The data were downloaded via the Tromsø Satellite Station. The SSM/I data and supporting files were provided by the EOS Distributed Active Archive Center (DAAC) at the National Snow and Ice Data Center, University of Colorado, Boulder, CO.

This project was partly funded by the partners of the Barents Sea Production Licenses 182, 225 and 228 (i.e., Norsk Hydro, Statoil, Chevron, Enterprise, Fortum, Agip and SDØE).

## Appendix A

Surface chlorophyll-*a* concentrations are measured by optical satellite instruments such as SeaWiFS (used in this paper) and Ocean Colour and Temperature Sensor (OCTS). Enhanced measurements is available from 2001 from National Aeronautics and Space Administration's (NASA's) MODerate resolution Imaging Spectrometer (MODIS) and probably from 2002 from European Space Agency's (ESA's) MEdium Resolution Imaging Spectrometer (MERIS). Sea Surface Temperature (SST) is available from infrared sensors such as the AVHRR (used in this paper) and the Along Track Scanning Radiometer (ATSR). MODIS now provides even more accurate SST data. ESA's Soil Moisture and Ocean Salinity (SMOS) instrument will offer sea surface salinity

estimates from ca. 2006. Daily sea ice concentrations have been available from the SSM/I instrument (used in this paper) since 1987. High-resolution sea ice imageries are also available from radars on board the satellites of ESA's ERS/Envisat and Canadian Space Agency's Radarsat.

## References


Aiken, J., Moore, G.F., Trees, C.C., Hooker, S.B., Clark, D.K., 1995. The SeaWiFS CZCS-type pigment algorithm. In: Hooker, S.B., Firestone, E.R. (Eds.), SeaWiFS Technical Report Series, vol. 29 NASA Goddard Space Flight Center, Greenbelt, MD, pp. 1–34.

Anker-Nilsen, T., Bakken, V., Strøm, H., Golovkin, A.N., Bianki, V.V., Tatarinkova, I.P., 2000. The status of marine birds breeding in the Barents Sea region. Norsk Polarinst. Rapportser., 113–213.

Carder, K.L., Chen, F.R., Lee, Z., Hawes, S.K., 1999. MODIS Ocean science team algorithm theoretical basis document: Case 2 Chlorophyll *a*, ATBD-MOD-19, Ver. 5.0. http://eospso.gsfc.nasa.gov/atbd/modistables.html.

Cavalieri, C., Parkinson, L., Gloersen, P., Zwally, H.J., 1997. Arctic and Antarctic sea ice concentrations from multichannel passive-microwave satellite data sets: October 1978 to September 1995, User's Guide. NASA Technical Memorandum 104627, 17 pp.

Clark, D.K., 1999. Algorithm theoretical basis document bio-optical algorithms—Case 1 waters, ATBD-MOD-18, Ver. 1.2, http://eospso.gsfc.nasa.gov/atbd/modistables.html.

Dutkiewicz, S., Follows, M., Marshall, J., Gregg, W.W., 2001. Interannual variability of phytoplankton abundances in the North Atlantic. Deep-Sea Res., Part II 48, 2323–2344.

Falk-Petersen, S., Sargent, J.R., Henderson, J., Hegseth, E.N., Hop, H., Okolodkov, Y.B., 1998. Lipids and fatty acids in ice algae and phytoplankton from the Marginal Ice Zone in the Barents Sea. Polar Biol. 20, 41–47.

Falk-Petersen, S., Pedersen, G., Kwasniewski, S., Hegseth, E.N., Hop, H., 1999. Spatial distribution and life-cycle timing of zooplankton in the marginal ice zone of the Barents Sea during the summer melt season in 1995. J. Plankton Res. 21, 1249–1264.

Falk-Petersen, S., Hop, H., Budgell, W.P., Hegseth, E.N., Korsnes, R., Løyning, T.B., Ørbæk, J.B., Kawamura, T., Shirasawa, K., 2000. Physical and ecological processes in the marginal ice zone of the northern Barents Sea during the summer melt period. J. Mar. Syst. 27, 131–159.

Gawarkiewicz, G., Plueddemann, A.J., 1995. Topography control of thermohaline frontal structure in the Barents Sea Polar Front on the south flank of Spitsbergen Bank. J. Geophys. Res. 100, 4509–4524.

Gloersen, P., Campbell, W.J., Cavalieri, D.J., Comaso, J.C., Parkinson, C.L., Zwalley, H.J., 1992. Arctic and Antarctic sea ice, 1978–1987. Satellite Passes: Microwave Observations and Analysis. Scientific and Technical Program NASA, Washington, 290 pp.

Haug, T., Nilssen, K.T., Øien, N., Potelov, V., 1994. Seasonal distribution of harp seals (*Phoca groenlandica*) in the Barents Sea. Polar Biol. 13, 163–172.

Hegseth, E.N., 1992. Sub-ice algal assemblages of the Barents Sea: species composition, chemical composition, and growth rates. Polar Biol. 12, 485–496.

Hegseth, E.N., 1997. Phytoplankton of the Barents Sea—the end of a growth season. Polar Biol. 17, 235–241.

Hegseth, E.N., 1998. Primary production of the northern Barents Sea. Polar Res. 17, 113–123.

Holm-Hansen, O., Mitchell, B.G., 1991. Spatial and temporal distribution of phytoplankton and primary production in the western Bransfield Strait region. Deep-Sea Res. 38, 961–980.

Holm-Hansen, O., Riemann, B., 1978. Chlorophyll *a* determination: improvements in methodology. Oikos 30, 438–447.

Hop, H., Poltermann, M., Lønne, O.J., Falk-Petersen, S., Korsnes, R., Budgell, W.P., 2000. Ice-amphipod distribution relative to ice density and under-ice topography in the northern Barents Sea. Polar Biol. 23, 357–367.

Joint, I., Groom, S.B., 2000. Estimation of phytoplankton production from space: current status and future potential of satellite remote sensing. J. Exp. Mar. Biol. Ecol. 250, 233–255.

Kögeler, J., Rey, F., 1999. Ocean colour and the spatial and seasonal distribution of phytoplankton in the Barents Sea. Int. J. Remote Sens. 20, 1303–1318.

Kögeler, J., Anselme, B., Falk-Petersen, S., 1995. Some applications of AVHRR and CZCS satellite data in studies of the Barents and Kara Seas. In: Skjoldal, H.R., Hopkins, C., Erikstad, K.E., Leinaas, H.P. (Eds.), Ecology of Fjords and Coastal Waters. Elsevier, Amsterdam, pp. 219–228.

Loeng, H., 1991. Features of the physical oceanographic conditions of the Barents Sea. Polar Res. 10, 5–18.

Lønne, O.J., Gulliksen, B., 1989. Size, age and diet of polar cod, *Boreogadus saida* (Lepechin 1773), in ice covered waters. Polar Biol. 9, 187–191.

Melnikov, I., 1997. The Arctic Sea Ice System. Gordon and Beach Science Publishers, Amsterdam, 204 pp.

Mobley, C.D., 1994. Light and Water: Radiative Transfer in Natural Waters. Academic Press, San Diego, 592 pp.

Moline, M.A., Prezelin, B.R., 2000. Optical fractionation of chlorophyll and primary production for coastal waters of the Southern Ocean. Polar Biol. 23, 129–136.

Morel, A., Antoine, D., Babin, M., Dandonneau, Y., 1996. Measured and modeled primary production in the northeast Atlantic (EUMELI JGOFS program): the impact of natural variations in photosynthetic parameters on model predictive skill. Deep-Sea Res. 43, 1273–1304.

National Snow and Ice Data Center, 1995. DMSP SSM/I brightness temperature and ice concentrations grids for the Polar Regions. User's guide, revised edition. NSIDC Distributed Active Archive Center, University of Colorado, Boulder.

Rey, F., Loeng, H., 1985. The influence of ice and hydrographic conditions on the development of phytoplankton in the Barents Sea. In: Gray, J.S., Christiansen, M.E. (Eds.), Marine Biology of Polar Regions and Effect of Stress on Marine Organisms. Wiley, London, pp. 49–63.

Sakshaug, E., 1997. Biomass and productivity distributions and their variability in the Barents Sea. ICES J. Mar. Sci. 54, 341–350.

Sakshaug, E., Skjoldal, H.R., 1989. Life at the ice edge. Ambio 18, 60–67.

Sakshaug, E., Slagstad, D., 1991. Light and productivity of phytoplankton in marine ecosystems: a physiological view. Polar Res. 10, 69–85.

Sathyendranath, S., Longhurst, A., Caverhill, C.M., Platt, T., 1995. Regionally and seasonally different primary production in the North Atlantic. Deep-Sea Res. 42, 1773–1802.

Smith, R.C., Dierssen, H.M., Vernet, M., 1996. Phytoplankton biomass and productivity in the western Antarctic Peninsula region. Antarct. Res. Ser. 70, 333–356.

Strass, V.H., Nöthig, E.M., 1996. Seasonal shifts in ice edge phytoplankton blooms in the Barents Sea related to the water column stability. Polar Biol. 16, 409–422.

Syvertsen, E.E., 1991. Ice algae in the Barents Sea: types of assemblages, origin, fate and role in the ice-edge phytoplankton bloom. Polar Res. 10, 277–288.

Sverdrup, H.U., 1953. On conditions of the vernal blooming of phytoplankton. J. Cons. Int. Explor. Mer 18, 287–295.

Vinje, T., 2001. Anomalies and trends of sea-ice extent and atmospheric circulation in the Nordic Seas during the period 1864–1998. J. Clim. 14, 255–267.

Vowinkel, E., Orvig, S., 1970. The climate of the north polar basin. In: Orvig, S. (Ed.), Climates of the Polar Regions. Elsevier, New York, pp. 129–226.

Wassmann, P., Slagstad, D., 1993. Seasonal and annual dynamics of carbon flux in the Barents Sea: a model approach. Polar Res. 13, 363–372.

Wiig, Ø., 1995. Distribution of polar bears (*Ursus maritimus*) in the Svalbard area. J. Zool. 237, 515–529.